Journal of Inflammation Research

Dovepress
open access to scientific and medical research

Open Access Full Text Article

ORIGINAL RESEARCH

Serpine1 Regulates Peripheral Neutrophil Recruitment and Acts as Potential Target in Ischemic Stroke

Zhijun Pu[1–5], Xinyu Bao[1–5], Shengnan Xia[1–5], Pengfei Shao[1–5], Yun Xu[1–5]

[1]Department of Neurology, Nanjing Drum Tower Hospital, Medical School and the State Key Laboratory of Pharmaceutical Biotechnology, Nanjing University, Nanjing, Jiangsu, 210008, People's Republic of China; [2]Institute of Brain Sciences, Nanjing University, Nanjing, Jiangsu, 210093, People's Republic of China; [3]Jiangsu Key Laboratory for Molecular Medicine, Medical School of Nanjing University, Nanjing, Jiangsu, 210008, People's Republic of China; [4]Jiangsu Province Stroke Center for Diagnosis and Therapy, Nanjing, Jiangsu, 210008, People's Republic of China; [5]Nanjing Neurology Clinic Medical Center, Nanjing, Jiangsu, 210008, People's Republic of China

Correspondence: Yun Xu, Email xuyun20042001@aliyun.com

Introduction: Peripheral neutrophil infiltration can exacerbate ischemia–reperfusion injury. We focused on the relationship between various peripheral immune cells and cerebral ischemia–reperfusion (I/R) injury.

Methods: In this study, we investigated the effects of dauricine on neuronal injury induced by ischemia–reperfusion and peripheral immune cells after ischemic stroke in mouse model, and we explored the undefined mechanisms of regulating peripheral immune cells through RNA sequencing and various biochemical verification in vitro and in vivo.

Results: We found that dauricine improved the neurological deficits of I/R injury, reduced the infarct volume, and improved the neurological scores. Furthermore, dauricine reduced the infiltration of neutrophils into the brain after MCAO-R and increased peripheral neutrophils but unchanged the permeability of the endotheliocyte Transwell system in an in vitro blood-brain barrier (BBB) model. RNA sequencing showed that chemotaxis factors, such as CXCL3, CXCL11, CCL20, CCL22, IL12a, IL23a, and serpine1, might play a crucial role. Overexpression of serpine1 reversed LPS-induced migration of neutrophils. Dauricine can directly bind with serpine1 in ligand–receptor docking performed with the Autodock and analyzed with PyMOL.

Conclusion: We identified chemotaxis factor serpine1 played a crucial role in peripheral neutrophil infiltration, which may contribute to reduce the neuronal injury induced by ischemia–reperfusion. These findings reveal that serpine1 may act as a potential treatment target in the acute stage of ischemic *stroke.*

Keywords: ischemia–reperfusion injury, dauricine, neutrophil recruitment, serpine1

Introduction

Stroke is a devastating disease with a high rate of death and a major cause of acquired disability in adults.[1] Ischemic *stroke* is the majority of *strokes*, but few curative therapeutic strategies are available. Thus far, tissue-type plasminogen activator and thrombectomy are the only clinically approved treatments for acute ischemic *stroke*, and there is substantial agreement between vascular neurology fellows.[2] However, the treatment time window is particularly important for ischemic *stroke*, within 0 to 4.5 h, which also limits the scope of application of tissue-type plasminogen activator and thrombectomy.

Peripheral immune cells have been widely reported to be activated and recruited into the ischemic hemisphere and exert elaborate functions, which is one of the key features of the neuroimmunological reaction to cerebral ischemia.[3,4] Among peripheral immune cells, neutrophils are the first to infiltrate the ischemic brain and are widely reported to play an important role in determining the outcome of ischemic *stroke*.[5] In the acute phase of post*stroke* inflammation, following the large release of inflammatory cytokines and chemokines, neutrophils are recruited into the ischemic

Received: 10 February 2022
Accepted: 7 April 2022
Published: 24 April 2022

hemisphere and exacerbate ischemic injury by damaging neural cells.[6] Inhibition of neutrophil infiltration, therefore, might represent a new therapeutic intervention for neuroprotection in the acute stages of ischemic *stroke*.[3,7]

Dauricine ($C_{38}H_{44}N_2O_6$) is an isoquinoline alkaloid and has rich pharmacological activity, including anti-Alzheimer's disease,[8,9] resistance to intracerebral hemorrhage and transient focal cerebral ischemia,[10,11] which are known mechanisms involved in antioxidative, antiapoptosis, and anti-inflammatory activities.[12,13] Dauricine is able to quickly pass through the blood-brain barrier, which is the material basis of neuroprotection.[14] Although these previous studies suggest the neuroprotection of dauricine in the transient middle cerebral artery and the potential medicinal value of dauricine, the neuron-immune actions and therapeutic prospects of dauricine in acute neuronal injury have not been investigated well.

In this study, we examined whether dauricine has potential ameliorative effects against brain I/R injury and investigated the underlying mechanisms in vivo, mainly focusing on the infiltration of peripheral immune cells into the brain by using an experimental model of focal cerebral ischemia–reperfusion.

Materials and Methods

Cell Culture and Treatment

Primary microglial cells were isolated and purified from 1-day-old C57BL/6J mice as described previously.[15] In brief, the cortexes of mouse were dissected on ice, digested with trypsin at 37°C, centrifuged and filtered to obtain glial cells. Then, cells were seeded in 75 cm^2 flasks and cultured for 10 days and 13 days at 37°C in a 5% CO_2 humidified atmosphere. Microglial cells were acquired by gently shaking the flasks and were replaced onto the indicated plates.

Dauricine was purchased from MUST (ChengDu, China, A0315), dissolved in DMSO for cell experiments, and dissolved in saline with 0.9% NaCl. Considering the limitation of drug administration capacity in mice and previous studies,[11,16] dauricine was dissolved in 0.9% NaCl saline with severe vortexing and finally presented as a turbid liquid. There are many studies of dauricine about transient focal cerebral ischaemia in rat and mouse, and the neuroprotective dose is from 5 to 10 mg/kg, so we chose the dosage of 10 $mg.kg^{-1}$ in this study.[16] After intragastric administration, the dosage was 10 $mg.kg^{-1}$, and the dosing capacity was 10 mL/kg. The first administration at reperfusion after focal cerebral ischemia within 30 min, once a day, continued until the end of the experiment. In vitro experiment on microglia cells, dauricine or vehicle pretreated for 1 h, then LPS (200 ng/mL) was added to stimulate the inflammation of microglia for 3 h, the detailed process is shown in Figure 1I.

Middle Cerebral Artery Occlusion in Mice

All animal protocols were conducted in strict accordance with the Guide for the Animal Care and Use Committee of Nanjing University, and passed the animal ethical review from the Experimental Animal Ethics Committee of Drum Tower Hospital Affiliated to Medical School of Nanjing University. Male C57BL/6J (B6) mouse (eight weeks old; body weight, 20 to 24 g) was obtained from the Animal Model Centre of Nanjing University. After anesthetizing with isoflurane, 6–0 surgical monofilament nylon sutures (Doccol Corporation, MA, USA) were introduced to obstruct the origin of the middle cerebral artery until the ipsilateral blood flow decreased to below 20% of baseline,[17,18] which is strictly monitored during the MCAO modeling using PeriFlux System 5000 (Perimed AB, Sweden), as shown in the Supplement 1A. After occlusion for 1 h, the blood flow was restored in the middle cerebral artery (MCA) region. The sham control mice underwent the same operation, without insertion of the filament into the MCA. The body temperature of all animals was monitored and maintained at 37.0°C to 37.5°C during the whole surgery. The cerebral blood flow is also measured by PeriCam PSI (Perimed AB, Sweden) at pre-operation (Supplement 1B) and post-operation (Supplement 1C), which help to judge the success of model or not. The mice were administered intragastrically with dose of dauricine or vehicle (10 mg.kg-1, 10 mL/kg) at reperfusion within 30 min after focal cerebral ischemia. At anatomy of other purpose, such as euthanasia, euthanasia of mice is applied with sodium pentobarbital (1%) at a dose of 45 mg/kg via intraperitoneal injection.

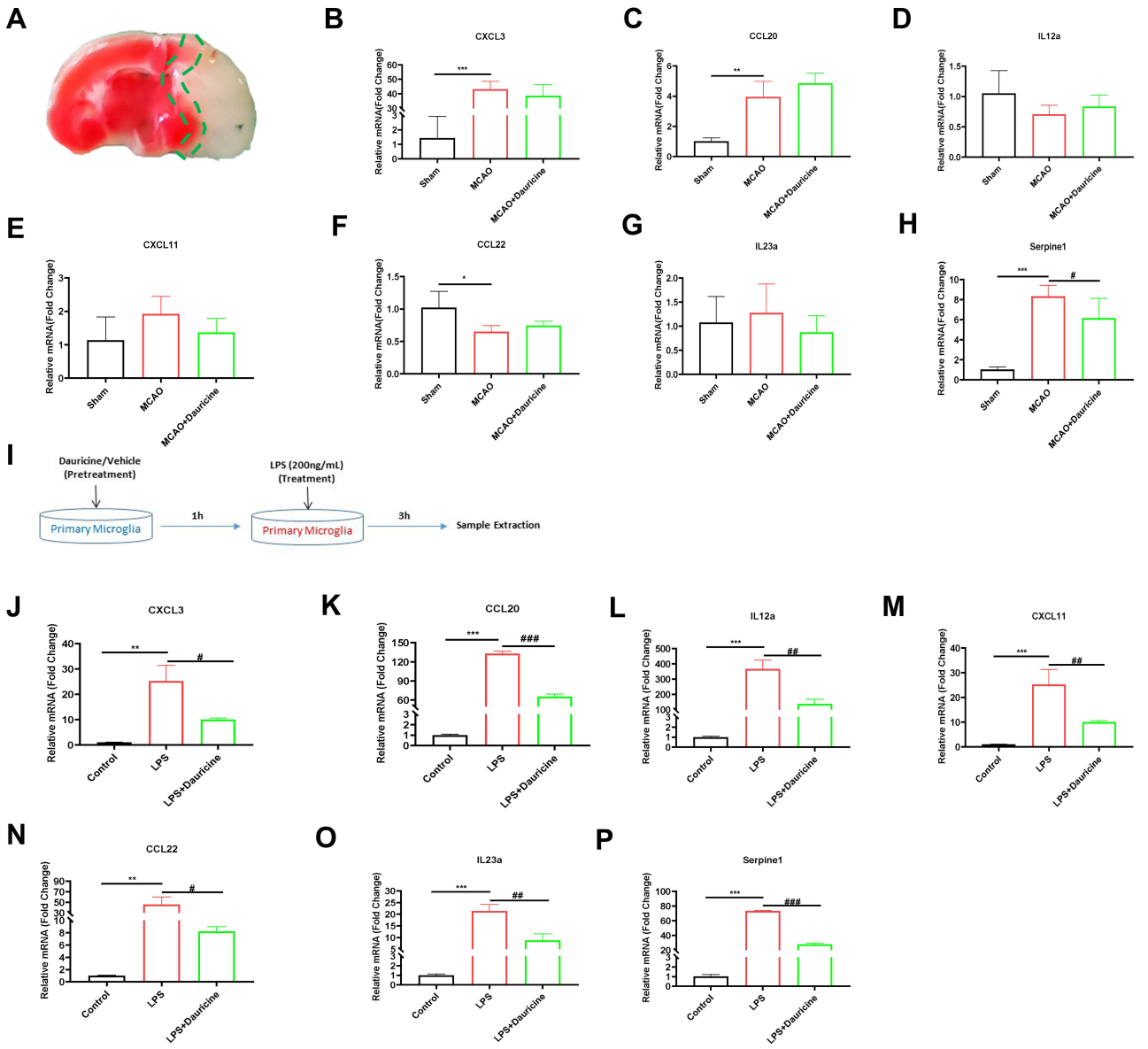

Figure 1 Serpine1 is the main chemotaxis factor for migration in vivo and in vitro. (**A**) Diagram of ischemia penumbra for sample. mRNA levels in the ischemia penumbra of tMCAO mice in the sham, MCAO and MCAO + dauricine groups were detected via quantitative real-time PCR (**B**–**H**). n = 5 mice per group. Sham group vs MCAO group, *p < 0.05, **p < 0.01, ***p < 0.001; MCAO group vs (MCAO + dauricine) group, $^{\#}$p < 0.05; unpaired Student's *t*-test. (**I**) Diagram illustrating drug administration and experimental design for primary microglia. mRNA levels in primary microglia in the control, LPS and LPS + dauricine groups were detected via quantitative real-time PCR (**J**–**P**). n = 5 per group. Control group vs LPS group, **p < 0.01, ***p < 0.001; LPS group vs (LPS + dauricine) group, $^{\#}$p < 0.05, $^{\#\#}$p < 0.01, $^{\#\#\#}$p < 0.001; unpaired Student's *t*-test.

Infarct Volume Calculation

To evaluate the infarct size of brain tissue, mice were euthanized 24 h after the induction of focal cerebral ischemia. The forebrains were quickly removed and sectioned coronally the main infarcted area into six serial 1-mm slices with relevant mouse mold (www.jkseiko.net, 1MM 0–175), which were then placed in 2% 2,3,5-triphenyltetrazolium chloride (TTC; Sigma–Aldrich) at 37°C for 20 min.[19] Digital images were obtained using a digital camera and analyzed by image-processing software (ImageJ version 1.8.0_172; National Institutes of Health, Bethesda, MD, USA), and infarct volume was calculated as a percentage of the volume of the bilateral side. Infarct volume was also calculated using the following formula: Percentage lesion volume (%) = (left hemisphere volume - right un-infarcted volume) / (left hemisphere volume x 2) x 100%.[20]

Neurological Deficit Scoring

Mice were evaluated for neurological function 24 h after MCAO as described previously,[21] including the modified neurological severity score (mNSS) test, rotarod test, and forelimb grip strength test. The mNSS test is a composite test of sensory function, motor function, reflexes and balance, and a higher score indicates more severe disease.[22] The rotarod test (IITC Life Science, USA) was used to assess motor deficits and sensorimotor coordination. The mice were trained continuously for three days before MCAO, and the time that the mice spent on the rod at a speed of 40 rpm was recorded after MCAO.[23] The forelimb grip strength test was performed with a grip strength meter (BIOSEB, USA), the strength of the grip prior to release was recorded in triplicate, and the average was counted.[24] The investigator who rated the mice was blinded to the experimental groups. The detailed process is shown in Figure 2A.

Brain Cell Isolation from Tissues and Flow Cytometric Assay

Mice were anesthetized and transcardially perfused with 40 mL cold PBS, and the ischemic half-brain tissue (ipsilateral to the MCAO) was isolated in 1x Dulbecco's modified Eagle's medium (DMEM) buffer (Gibco, Thermo Fisher, China) containing 4.5 g/L D-glucose and 10% fetal calf serum (FBS). Single-cell suspensions were obtained using a manual grinder, and the total mixture obtained was passed through a 70 μm pore filter and then stratified on a 30–70% Percoll gradient (Cytiva, Sweden, 17089101). Gradient centrifuging at 2000 rpm for 20 min (up 1, down 0), cell appeared around the interface, then collected and incubated with the fluorophore-labeled primary antibodies as follows: rat anti-mouse CD45 (Bio-Legend, Clone 30-F11, PE-cy7, 1:2000), CD11b (Invitrogen, Clone M1/70, AF488, 1:400), CD4 (Invitrogen, Clone RM4-5, APC, 1:400), CD8 (Invitrogen, Clone 53-6.7, Perp-cy5.5, 1:400), Ly6G (Invitrogen, Clone 1A8-Ly6 g, PE, 1:400), Ly6C (Bio-Legend, Clone HK1.4, BV421, 1:400), F4/80 (Bio-Legend, Clone BM8, 1:400), B220 (Bio-Legend, Clone RA3-6B2, 1:400). Data acquisition was carried out in a BD LSRFortessa cell analyzer (BD Biosciences, San Jose, CA, USA) using FacsDiva software (BD Biosciences), and data analysis was adopted with FlowJo software (version 10.5.3, Tree-Star Inc., Ashland, OR, USA).

Peripheral Immune Cell Isolation from Blood and Flow Cytometric Assay

Mice were anesthetized, and peripheral blood was sampled from mouse eyes with tubes containing EDTA. Then, 1 mL ACK lysis buffer (Gibco, A10492-01, USA) was added to every tube to destroy red blood cells, fully mixed, and centrifuged at 2000 rpm for 5 min. Finally, peripheral immune cells were acquired. Incubation with fluorophore-labeled primary antibodies, data acquisition, and analysis were performed as described above.

Immunofluorescence Staining and Cell Counting in Brain Sections and Microglia Cells

Mice were deep anesthetized and then perfused with PBS and 4% paraformaldehyde (PFA). Followed with soaking in 4% paraformaldehyde for overnight, the brains were dehydrated in 15% and 30% glucose solutions.[25] Brains were sectioned at the thickness of 20 μm with a freezing microtome (Thermo Scientific, CryoStar NX50 HOP). Brain slices or microglia cell fixed in 4% PFA for 15 min at room temperature, permeabilized with 0.25% Triton X-100 for 20 min, then blocked in blocking buffer with 2% bovine serum albumin for 2h, followed by incubating with indicated primary antibodies (Ly6G, CST, 87048, 1:200; Serpine1, Santa, SC-5297, 1:100) overnight at 4°C. On the second day, being washed 3 times with PBS, and then the slices were incubated with corresponding secondary antibodies with 570 nm wavelength (1:500, Invitrogen, Carlsbad, CA, USA) at room temperature for 2 h, avoiding light. The nuclei were counterstained with a DAPI staining kit (1:1000, Bio-world). Images were obtained using a fluorescence microscope (Olympus X73, Fukasawa, Japan), and positive amount was quantified with Image-J software (https://imagej.nih.gov/ij/, NIH, Bethesda, USA).

Neutrophil Isolation from Marrow and Migration Model

Neutrophils were collected from the bone marrow of mice as described previously.[26] Briefly, femora and tibia of mice were separated, bone marrow cells were acquired, red cells were cleared with ACK lysis buffer, and stained with ultrapure anti-Ly-6G microbeads (Miltenyi Biotec, 130-120-337, 1:100). Finally, neutrophils were isolated by magnetic separation.

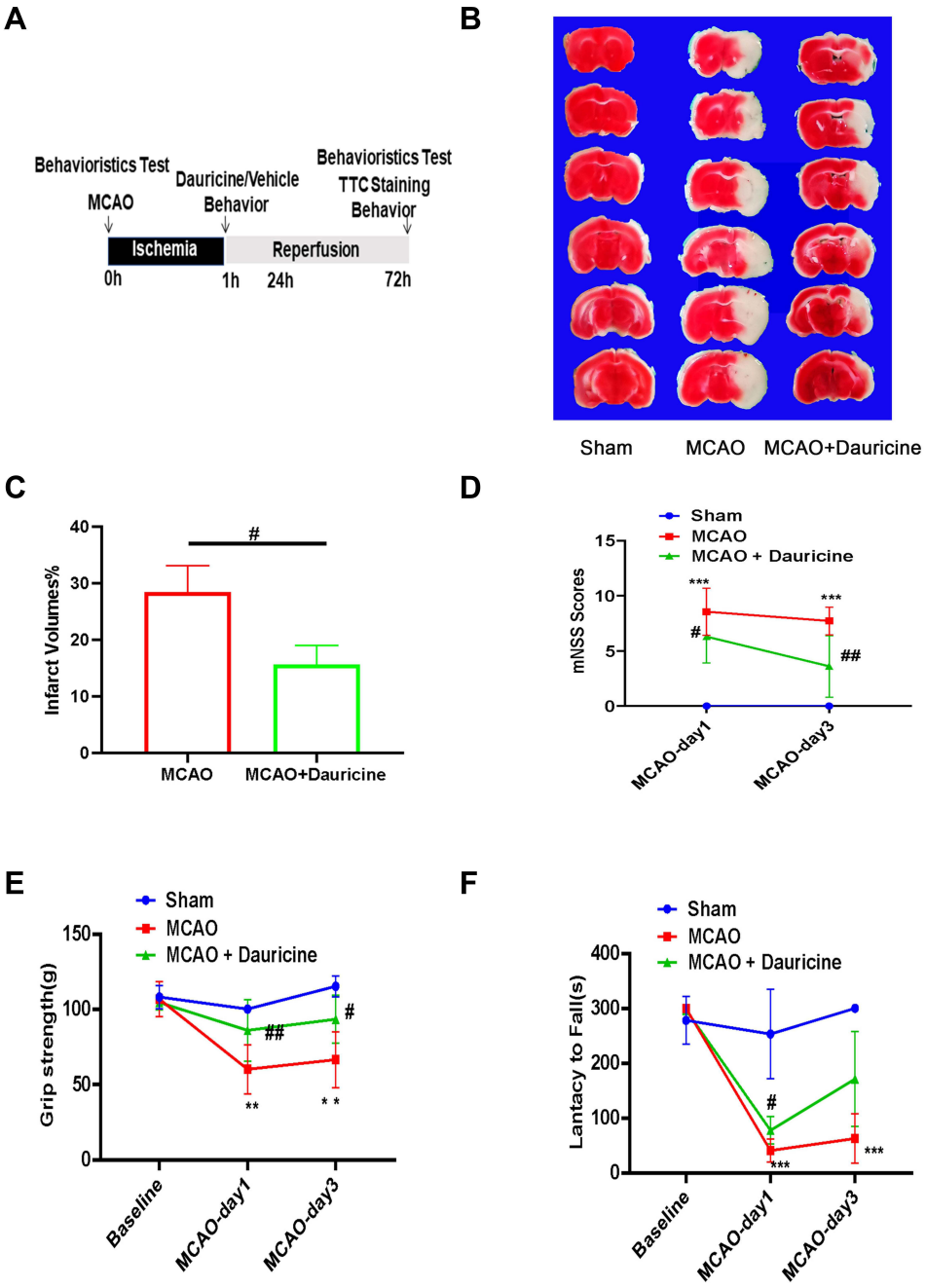

Figure 2 Dauricine decreases the brain infarct size and neurological deficits after tMCAO injury. (**A**) Flowchart illustrating drug administration and experimental design. (**B**) Mouse brains were procured at 24 h after ischemia–reperfusion, and TTC staining was applied to determine the infarct volume and quantified (**C**). (**D**) mNSS Scores, (**E**) grip strength and (**F**) lantacy to fall were applied to evaluate the functional outcomes of the two groups of tMCAO mice. n = 5 mice per group. Sham group vs MCAO group, $^{**}p < 0.01$, $^{***}p < 0.001$; MCAO group vs (MCAO + dauricine) group $^{\#}p < 0.05$, $^{\#\#}p < 0.01$, one-way ANOVA with Bonferroni post hoc test.

The in vitro neutrophil migration model was constructed as described previously with some simplification.[27] Primary microglia were cultured in 24-well plates and transfected with serpine1 overexpression or vector plasmid for 48 h. Then, primary microglia were treated with LPS (200 ng/mL) or dauricine (1 μM), and 24-well Transwells seeded with DiO-strained (Beyotime, C1038, 3,3′-dioctadecyloxacarbocyanine perchlorate) neutrophils were transferred into primary microglia plates for 3 h. Migrated neutrophils on the underside of the plate were detected by fluorescence microscopy (excitation 488 nm, emission 501 nm). The detailed process is shown in Figure 3A.

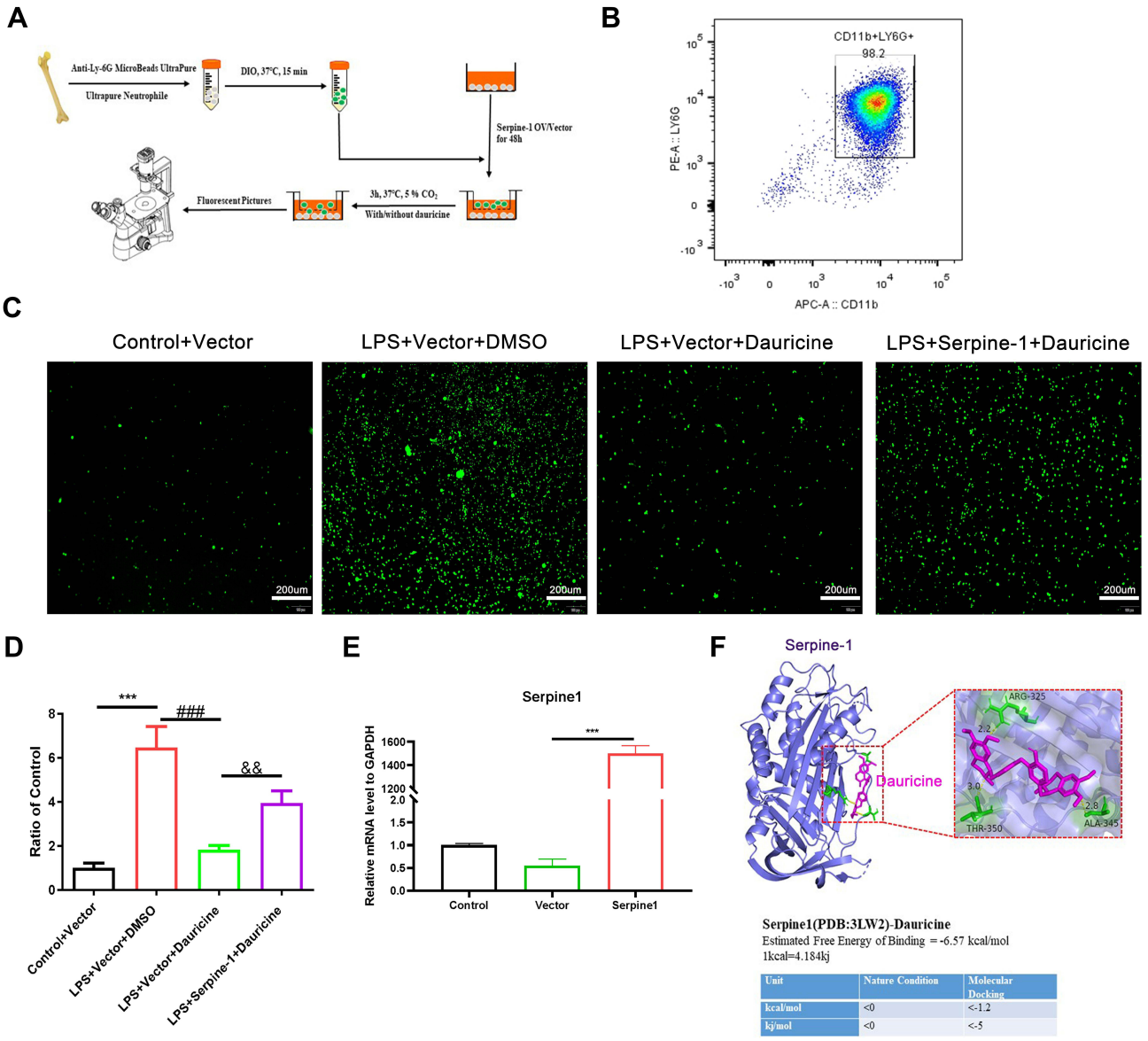

Figure 3 Serpine1 reversed the chemotaxis inhibition of dauricine on neutrophils. (**A**) Diagram of primary neutrophils from the bone marrow of mice. (**B**) The purity of primary neutrophils isolated from the bone marrow of mice was detected by flow cytometry with APC-CD11b and PE-Ly6G antibodies. (**C**) mRNA expression of serpine1 was detected via quantitative real-time PCR after 48 h of plasmid transfection in primary microglia. n = 3 mice per group. Vector group vs serpine1 overexpression group, ***p < 0.001; unpaired Student's *t*-test. (**D**) Primary neutrophils were prestrained with DiO (cell membrane green fluorescent probe) and then migrated for 3 h with an inducer from microglia. Representative pictures of DiO-stained primary neutrophil migration for 3h from the control+vector, LPS+vector+DMSO, LPS+vector+dauricine, and LPS+serpine1+sauricine groups and were counted (**E**), n = 5 per group. Control+vector vs LPS+vector+DMSO group, ***p < 0.001; LPS+vector+DMSO vs LPS+vector +dauricine group, ###p < 0.001; LPS+vector+dauricine vs LPS+serpine1+dauricine group, &&p < 0.01; unpaired Student's *t*-test. (**F**) Ligand receptor docking was performed with AutoDock and analyzed with PyMOL. The top panel shows the joint diagram of dauricine and serpin-1 protein. The lower panel shows the energy data under natural conditions and molecular docking.

Measurement of TEER

The TEER of the bEnd.3 monolayer is an accepted indicator of permeability in an in vitro BBB model. bEnd.3 cells were seeded in the transwell to simulate the blood–brain barrier, and the TEER was measured after 24 h reperfusion following OGD with a portable endothelial voltohmmeter (EVOM, World Precision Instruments, Sarasota, FL, USA) according to the manufacturer's instructions.

FITC-Dextran Transendothelial Permeability Assay

The integrity of the endothelial monolayer is another indicator of permeability in an in vitro BBB model. The FITC-dextran transendothelial permeability assay of the bEnd.3 monolayer was assessed in the Transwells. FITC-dextran (MW,

70,000, Sigma–Aldrich, FD70S) was added to the upper compartment after 24 h of reperfusion following OGD and incubated for 30 min, and 100 μL of supernatant from the lower chamber was analyzed via a microplate reader (excitation 490 nm, emission 520 nm).

Quantitation of BBB Permeability

BBB permeability was assessed by the Evans blue (EB) extravasation assay. Mice were injected with EB (2% in 0.9% saline; 8 mL/kg, Sigma-Aldrich, E2129) via the tail vein. Six hours later, mice were anesthetized and transcardially perfused with 40 mL cold PBS, then the brains were cut into slices for analysis and photograph. Each hemisphere was weighed and homogenized in N, N-dimethyl formamide (Biosharp) with 1mL/100mg, then centrifuged at 14,000 rpm for 45 min, and the EB concentration in the supernatant was determined with a microplate reader Spark® (Tecan, Austria) at 620 nm. The EB extravasate was expressed as micrograms per gram of wet tissue.[21]

RNA Sequence

The sequence was performed by Majorbio of Shanghai, China. Briefly, total RNA was isolated from samples, and mRNA was enriched from total RNA according to the polyA selection method by oligo (dT) beads and then fragmented by fragmentation buffer first. Next, the mRNA was randomly fractured by fragmentation buffer, and small fragments of approximately 300 bp were separated by magnetic bead screening. Second, double-stranded cDNA was synthesized using a SuperScript double-stranded cDNA synthesis kit (Invitrogen, CA) with random hexamer primers (Illumina). Then, the synthesized cDNA was subjected to end repair, phosphorylation and "A" base addition according to Illumina`s library construction protocol. Finally, an RNA-sequence transcriptome library was prepared following the TruSeq™ RNA sample preparation kit from Illumina (San Diego, CA) using 1 μg of total RNA.

RNA Isolation and Quantitative Real-Time PCR

Cortical penumbra tissue and cell samples were lysed with TRIzol reagent (Invitrogen), total RNA was extracted according to the manufacturer's protocol, and the quality of the RNA was assessed with a Nanodrop 2100 spectrophotometer (Agilent). Reverse transcription from RNA to cDNA was performed with the PrimeScript RT regent kit (Vazyme, Nanjing, China, R323-01). Quantitative real-time PCR was performed in a Roche LightCycler® 96 system (Roche, Mannheim, Germany) with a SYBR green kit (Accurate, Wuhan, China, AG11701). The primers are as follows:

CXCL3: forward primer- CCAGACAGAAGTCATAGCCAC, reverse primer-CTTCATCATGGTGAGGGGCTT;

CXCL11: forward primer- GGCTTCCTTATGTTCAAACAGGG; reverse primer- GCCGTTACTCGGGTAAA TTACA;

CCL20: forward primer- GCCTCTCGTACATACAGACGC, reverse primer- CCAGTTCTGCTTTGGATCAGC;

CCL22: forward primer- AGGTCCCTATGGTGCCAATGT; reverse primer- CGGCAGGATTTTGAGGTCCA;

IL12a: forward primer- CTGTGCCTTGGTAGCATCTATG; reverse primer- GCAGAGTCTCGCCATTATGATTC;

IL23a: forward primer- ATGCTGGATTGCAGAGCAGTA; reverse primer- ACGGGGCACATTATTTTTAGTCT;

Serpine1: forward primer- TTCAGCCCTTGCTTGCCTC; reverse primer- ACACTTTTACTCCGAAGTCGGT;

GAPDH: forward primer- AGGTCGGTGTGAACGGATTTG, reverse primer-TGTAGACCATGTAGTTGAGGTCA;

β-actin: forward primer- GGCTGTATTCCCCTCCATCG, reverse primer- CCAGTTGGTAACAATGCCATGT.

Ligand–Receptor Docking and Analysis

Ligand–receptor docking was performed with the AutoDock 4 program distributed with AutoDock, version 4.2.6. The binding site was analyzed, and images were generated with PyMOL, version 2.2.0.[28] The serpine1 3D protein structure is from PDB (Protein Data Bank, www.rcsb.org). The dauricine 3D structure is from PubChem (pubchem.ncbi.nlm.nih.gov).

Statistical Analysis

All values are expressed as the mean ± SEM, and the quantitative variables were statistically analyzed using Student's two-tailed *t*-test for two-group comparisons and one-way ANOVA followed by Dunnett's test for multiple pairwise

comparisons. P < 0.05 was considered statistically significant. All statistical analyses were performed using GraphPad Prism 5 software (GraphPad Software, San Diego, CA, USA).

Results

Dauricine Decreases Brain Infarct Size and Neurological Deficits After tMCAO Injury

We examined whether the administration of dauricine would reduce infarct volume and improve neurological deficits, and the process scheme was carried out as shown in Figure 2A. Mice developed an infarction affecting the right hemisphere after 1 h of MCAO, followed by reperfusion at 1 day and 3 days. TTC staining was performed to evaluate the cerebral infarct volume. Compared to the vehicle-treated group, the administration of dauricine showed a 45% reduction in infarct volume at 1 day after MCAO (Figure 2B and C; $P < 0.05$; one-way ANOVA followed by Dunnett's test). As shown in Figure 2D–F, the group treated with dauricine had significantly better neurological function at 24 h after MCAO than the vehicle-treated group ($P < 0.05$; Wilcoxon signed-rank test).

Dauricine Attenuates Neutrophil Infiltration into the MCAO-R Brain

It is known that the infiltration of peripheral immune cells into the brain increases neuronal damage in the acute phase of tMCAO reperfusion.[26,29] To explore the effects of dauricine on the accumulation of peripheral immune cells, including CD4+ T cells, CD8+ T cells, macrophages, monocytes, B cells, and neutrophils, in the ischemic brain were assessed via flow cytometry (Figure 4A). The ratios of CD4+ T cells, CD8+ T cells, macrophages, monocytes, B cells, and neutrophils in the ischemic hemisphere of tMCAO mice were comparable between the sham group. Compared to the sham group, it showed a significant increase in neutrophil, monocyte and CD8+ T cells infiltration, consistent with previous reports,[29–31] and CD4+ T cell, macrophage, and B cell decreased after MCAO. However, only the mice administered dauricine showed a significant reduction in neutrophils (Figure 4B; $P < 0.001$; one-way ANOVA followed by Dunnett's test), and it was verified by the histo-immunofluorescence (Figure 5A–D), which might partly account for the dauricine-induced protective effects. CD4+ T cells, CD8+ T cells, macrophages, monocytes, and B cells were not shown here (Supplement 2A–F).

Dauricine Enhances Peripheral Immune in Blood

To verify whether dauricine reduced neutrophils into the ischemic hemisphere by reducing the ratio of peripheral immune cells in blood, peripheral blood was collected, and peripheral immune cells were detected by flow cytometry (Figure 4C). Compared with the MCAO group, the dauricine group had a significantly increased neutrophil ratio, which indicated that dauricine attenuated neutrophil infiltration but not via a reduction in peripheral neutrophils and that dauricine might enhance peripheral immunity (Figure 4D). CD4+ T cells, CD8+ T cells, macrophages, monocytes, and B cells were also detected, and shown in Supplement 2G–L.

Dauricine Fails to Recover the Disruption of BBB

To verify whether dauricine reduces neutrophils into the ischemic hemisphere by restoring the disruption of the BBB, we assessed the permeability of the endotheliocyte Transwell system in an in vitro BBB model. Fluorescein isothiocyanate (FITC)-labeled dextran leakage and transendothelial electrical resistance (TEER) in the Transwell system remained unchanged upon dauricine treatment, which also excluded the possibility that dauricine attenuated neutrophil infiltration through THE reduction of peripheral neutrophils by repairing BBB damage (Figure 4E and F). The BBB permeability in vivo was assessed by the Evans blue (EB) extravasation assay, and shown in Supplement 3A–C.

Dauricine Decreases Chemotaxis Factors Expression

To further explore why dauricine reduces neutrophils into the ischemic hemisphere, RNA sequencing was applied. As shown in Figure 6A, compared with the LPS group, the dauricine group had 542 upregulated genes and 313 down-regulated genes (pad-just ≤ 0.05, fold ≥ 1.5). GO enrichment analysis between the LPS group and dauricine group revealed the common key words 'chemotaxis' from 3 to 20 enrichment differential gene sets (Figure 6B) (pad-just ≤

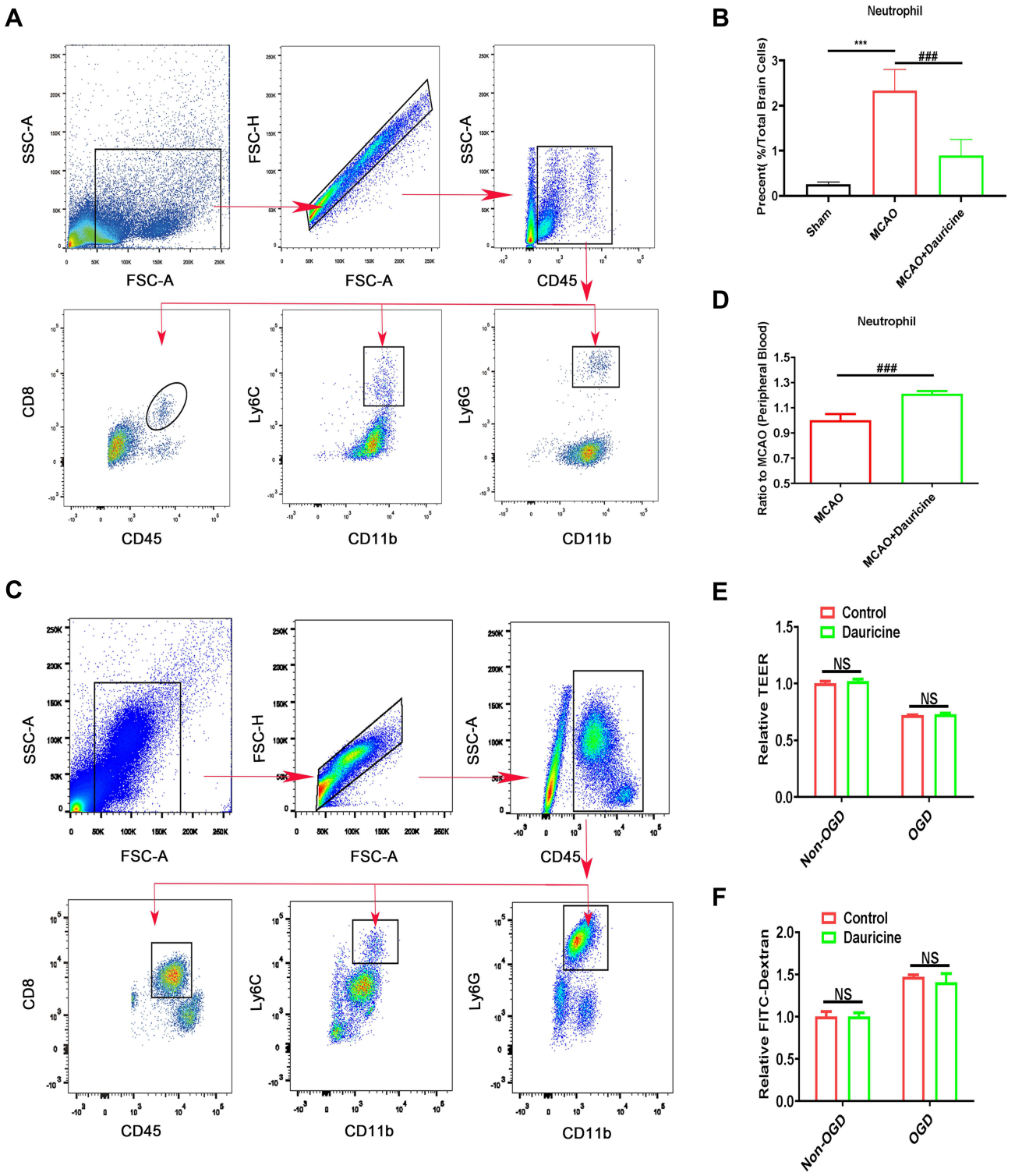

Figure 4 Dauricine attenuates neutrophil infiltration into the MCAO-R brain, enhances peripheral immunity in blood, but fails to recover the disruption of the BBB. (**A**) Gating strategy for infiltrating immune cells isolated from the ischemic brain after tMCAO. Counts of neutrophils (**B**) in the brains of the control and dauricine groups of tMCAO mice. (**C**) Gating strategy for infiltrating immune cells isolated from the blood after tMCAO. Counts of neutrophils (**D**) in the blood of the control and dauricine groups of tMCAO mice. (**E**) Dextran leakage was detected by a microplate reader, with the dextran leakage in the control group without OGD-R treatment normalized to 1. (**F**) Mean TEER values were measured using a voltohmmeter, with the TEER in the control group without OGD-R treatment normalized to 1. n = 3 per group. NS., no significance ($p > 0.05$). Sham group vs tMCAO group, ***$p < 0.001$; MCAO group vs (MCAO + dauricine) group, $^{###}p < 0.001$; unpaired Student's *t*-test.

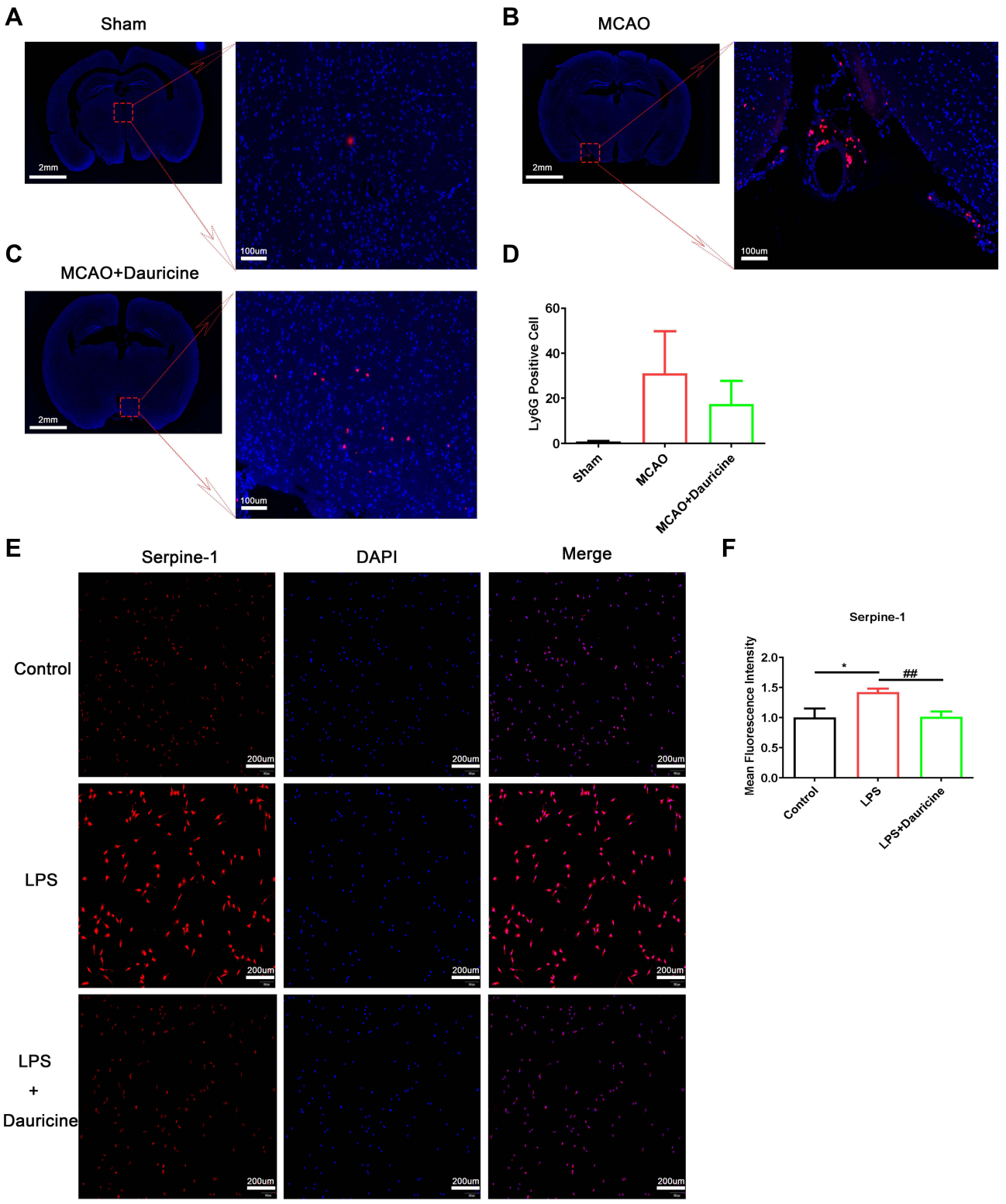

Figure 5 Dauricine reduces neutrophil infiltration into the MCAO-R brain, and inhibits the serpine1 activity and expression. Immunofluorescence staining of ly6G protein in mouse slices of sham (**A**), MCAO (**B**) and MCAO + dauricine (**C**), and the ly6G positive cells were counted (**D**). Microglia cell induced by LPS or dauricine for 3h, and stained with serpine1 and DAPI (**E**), mean fluorescence intensity of serpine1 was counted (**F**). n = 5 per group. Control group vs LPS group, *$p < 0.05$; LPS group vs (LPS + dauricine) group, $^{\#\#}p < 0.01$; unpaired Student's *t*-test.

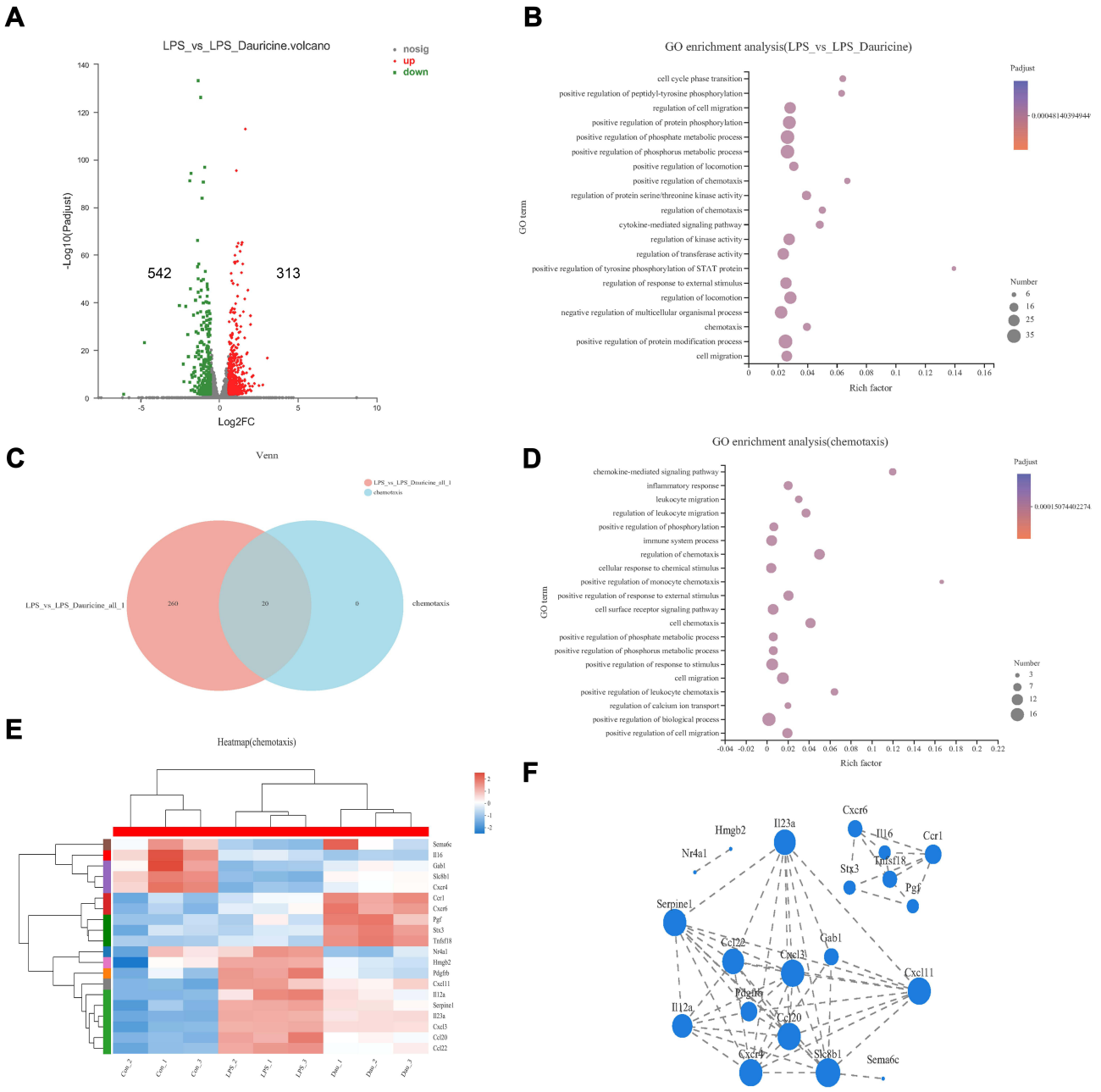

Figure 6 Dauricine treatment affects the expression of chemotaxis factors. (**A**) Volcano plots displaying variations in mRNA expression in LPS-stimulated primary microglia between the LPS and LPS + dauricine groups. n = 3 per group. (**B**) GO enrichment analysis between the LPS and LPS + dauricine groups. (**C**) Venn analysis between the LPS vs LPS + dauricine and chemotaxis sets. (**D**) GO enrichment analysis of chemotaxis set. (**E**) Heatmap of chemotaxis in the control, LPS, and LPS + dauricine groups. (**F**) Visual analysis of protein interaction network relationships of chemotaxis set.

0.05, top 20), which were 'positive regulation of chemotaxis', "regulation of chemotaxis" and "chemotaxis", including 20 genes (Figure 6C). GO enrichment analysis of "chemotaxis" and found the main enrich was "chemokine-mediated signaling pathway" (Figure 6D) (pad-just ≤ 0.05, top 20). Integrating three chemotaxis gene sets, we obtained 20 genes and drew a heatmap of chemotaxis (Figure 6E) (soft: RSEM; expression index: TPM). STRING database (http://string-db.org/) was used to analyze the protein interaction network of those genes, and network-X of Python was used to visualize the network of those genes to obtain the protein interaction network relationship (Figure 6F) (pad-just ≤ 0.05; correlation coefficient: 0.8; correlation algorithm: spearman).

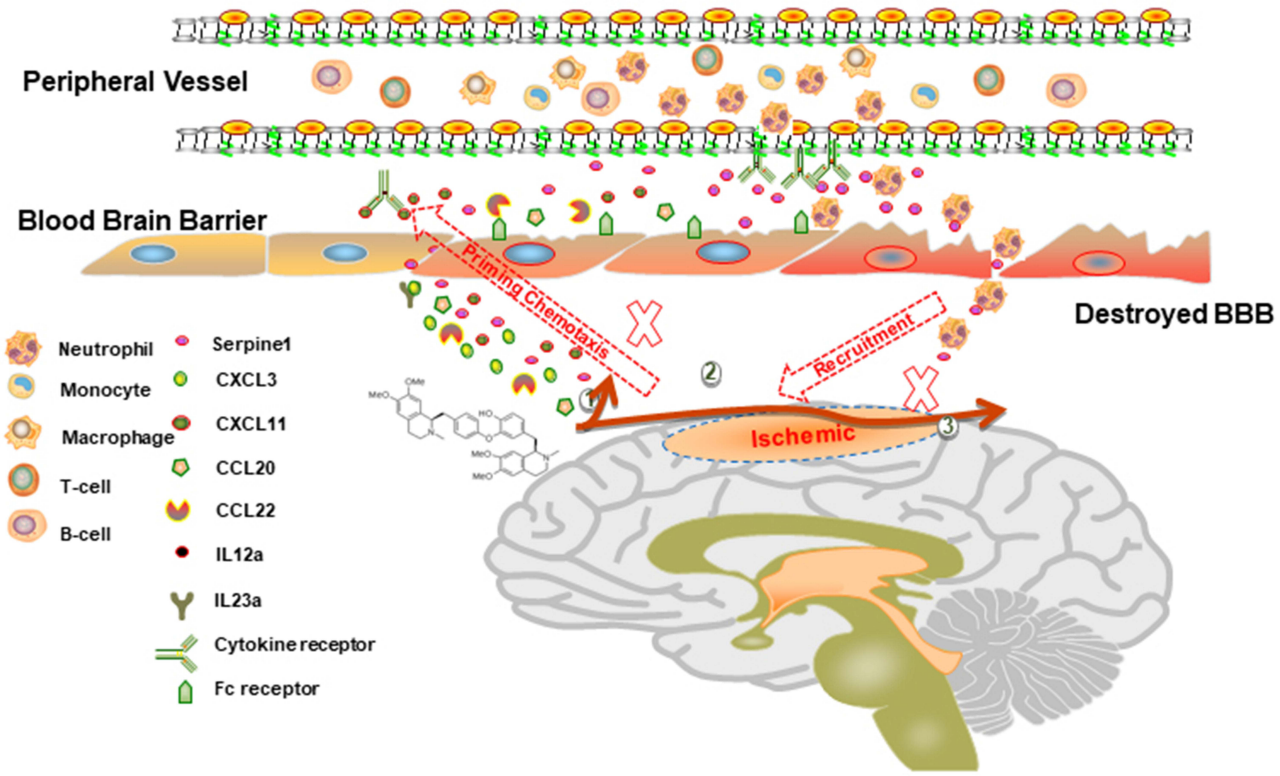

Figure 7 Schematic diagram of the proposed mechanisms underlying the role of dauricine combined with serpine1 on neutrophil infiltration in ischemic stroke.

Serpine1 is the Main Chemotaxis Factor for Neutrophil Migration

By analyzing the heatmap of chemotaxis, we selected the significantly variational genes that were CXCL3, CXCL11, CCL20, CCL22, IL12a, IL23a and serpine1. Subsequently, we applied quantitative real-time PCR to validate their expression in the samples from ischemic penumbra of tMCAO mice (Figure 1A) and primary microglia (Figure 1I). Validation in vitro and in vivo (Figure 1B–P) showed that only serpine1 expression was consistent, the others factors such as CXCL3, had the same trend, but no so significant in vivo, which is the reason why we chose the serpine1 as the research object. Cytokine works mainly through protein in microenvironment, so protein expression of serpine1 with immunofluorescence was also detected (Figure 5E and F), and the tendency is consistent with gene expression. Therefore, serpine1 might be the main factor that dauricine works, and we surmised that serpine1 was related to neutrophil migration.

Serpine1 Reversed the Migration of Neutrophils

We constructed an in vitro model of primary neutrophil migration and constructed a direct communication platform between neutrophils and microglia (Figure 3A). The purity of primary neutrophils isolated from the bone marrow of mice was up to 98.2% (Figure 3B). Serpine1 overexpression significantly increased after 48 h of plasmid transfection (Figure 3E). Consistent with previous results and surmise, dauricine significantly reduced the LPS-induced migration of neutrophils, but overexpression of serpine1 reversed this reaction (Figure 3C and D).

Dauricine Direct Joined with Serpine1

Ligand–receptor docking was performed with AutoDock and analyzed with PyMOL. The molecular docking energy (<-1.2 kcal/mol) was low enough, which demonstrated that dauricine can directly bind with serpine1 (Figure 3F).

Discussion

In this study, we found that dauricine significantly reduced the infiltration of peripheral immune cells, especially neutrophils, into the I/R brain after 24 h. This is the first study to focus on the pharmacological activity of dauricine in neuroimmunity and I/R injury. Dauricine has anti-inflammatory activity;[13] however, the origin of inflammatory factors and the relationship between neuroimmunity and peripheral immunity are unknown. Immune cells are the bridge between neuroimmunity and peripheral immunity. Neutrophils are rapidly recruited in response to local tissue infection or inflammation, and recent research found that neutrophil extravasation at the leptomeninges was also detected in experimental animal models and the human tissue of ischemic *stroke*.[29] Neutrophil extracellular trap formation induced in the cerebral ischemic brain might aggravate inflammation and brain damage.[32] Furthermore, neutrophils can release further proinflammatory factors and chemotactic agents, recruit more neutrophils and exacerbate inflammation.[33] Therefore, we hypothesized that dauricine attenuated neuronal injury induced by cerebral ischemia–reperfusion and that its mechanisms are, at least in part, due to suppression of neutrophil recruitment (Figure 7).

Many previous studies have revealed the neuroprotective effects of dauricine in chronic and acute CNS diseases. In chronic CNS diseases, such as Alzheimer's disease, dauricine enhances ER-associated degradation by activating X-box binding protein 1, accelerates the degradation of amyloid-beta, has antioxidative and antiapoptotic pharmacological activity in a Caenorhabditis elegans model of Alzheimer's disease, and enhances mitochondrial function to attenuate spatial memory impairment and Alzheimer's disease in 3xTg-AD mice.[8,9,12,34] In acute neuronal injury, dauricine alleviates secondary brain injury after intracerebral hemorrhage and inhibits apoptosis and ferroptosis of nerve cells.[10,35] However, the pharmacological activity of dauricine in I/R injury and neuroimmunity remains unclear.

In the present study, it was demonstrated that the administration of dauricine significantly attenuated neuronal injury following I/R, which might be related to the suppression of neutrophil infiltration into the brain. How does dauricine reduce neutrophil infiltration into the I/R brain? There might be three factors: (1) The change in BBB integrity. The BBB could be damaged within the thrombolytic time window and is considered to be a precursor to hemorrhagic transformation during reperfusion, in which disruption can cause many harmful substances and cells to enter the brain and worsen damage.[36] Our results indicated that dauricine has no effect on the BBB, so the reduction in neutrophil infiltration is not due to the change in the BBB. (2) The number and ratio of neutrophils in peripheral blood. Peripheral immunosuppression is induced in *stroke* and characterized by decreased splenocyte numbers and proliferation and altered percentages of immune cells in peripheral blood.[37] Our results showed that intragastric administration of dauricine improved peripheral immunity and increased neutrophils rather than reducing neutrophils in peripheral blood. (3) Chemokine is released from the brain. It is well known that inhibition of inflammatory cell accumulation in the brain may lead to amelioration of ischemic injury at the early stage of *stroke*. Chemokines do not induce neurodegeneration directly, but chemokines may be a potential target for future therapies reducing inflammatory cell migration to the brain in early *stroke*.[38] We explored neutrophil-related chemokines and found that dauricine indeed reduced the expression of the chemokine serpine1 in the ischemic penumbra at 24 h postischemia reperfusion. This might be a reasonable explanation for why dauricine reduced neutrophil infiltration into the brain.

Serpine 1, a primary inhibitor of tissue-type plasminogen activator (PLAT), is required for fibrinolysis downregulation and is responsible for the controlled degradation of blood clots. Baseline serpine1 gene methylation might be a predictor of weight loss after laparoscopic sleeve gastrectomy (LSG), and postoperative serpine1 protein could be a predictor of weight loss maintenance.[39] Serpine1 is not merely a marker of senescence but is both necessary and sufficient for the induction of replicative senescence downstream of p53.[40] Elevation of serpine1 contributes importantly to ATII cell senescence in fibrotic lung diseases and to the activation of the p53-p21-Rb cell cycle repression pathway.[41] In a study of plasma samples from 40 patients with venous thrombosis, several miRNAs directly interacted with serpine1 mRNA at rs1050955 and affected serpine1 serpine1 protein levels, which could be envisaged as a biomarker for inflammatory and thrombotic disorders.[42] Serpine1, a PLAU inhibitor, is involved in the regulation of cell adhesion and spreading. In our study, serpine1 acted as a regulator of peripheral neutrophil migration, independent of its role as a protease inhibitor, which has not been well covered. Dauricine can directly bind with serpine1, which might inhibit activity and expression of serpine1. Here, we provide some explanations based on our limited data, hope more attention

will be given to serpine1 in stroke, and more evidence such as conditional knockout mice of serpine1 is needed to clarify it important function on ischemic stroke in the future.

Conclusion

The potential pharmacological effects of dauricine in ischemic *stroke* have been confirmed using both in vivo and in vitro experimental models of cerebral I/R injury. These effects are, at least in part, due to inhibition of neutrophil infiltration through reduction of chemokines serpine1 in the ischemic penumbra. The current findings indicate that the peripheral immune effect of dauricine may prove beneficial and that serpine1 may act as a potential treatment target in the acute stage of ischemic *stroke*.

Acknowledgments

This research was supported by the National Natural Science Foundation of China (81920108017, 82130036, 81630028) and the Key Research and Development Program of Jiangsu Province of China (BE2020620). Jiangsu Province Key Medical Discipline (ZDXKA2016020).

Disclosure

All authors claim that there are no conflicts of interest and that none of the authors' institutions has contracts relating to this research through which it may stand to gain financial support now or in the future.

References

1. Virani SS, Alonso A, Aparicio HJ, et al. Heart disease and stroke statistics-2021 update: a report from the American Heart Association. *Circulation*. 2021;143:e254–e743. doi:10.1161/CIR.0000000000000950
2. Ramadan AR, Denny MC, Vahidy F, et al. Agreement among stroke faculty and fellows in treating ischemic stroke patients with tissue-type plasminogen activator and thrombectomy. *Stroke*. 2017;48:222–224. doi:10.1161/STROKEAHA.116.015214
3. Jin R, Yang G, Li G. Inflammatory mechanisms in ischemic stroke: role of inflammatory cells. *J Leukoc Biol*. 2010;87:779–789. doi:10.1189/jlb.1109766
4. Macrez R, Ali C, Toutirais O, et al. Stroke and the immune system: from pathophysiology to new therapeutic strategies. *Lancet Neurol*. 2011;10:471–480. doi:10.1016/S1474-4422(11)70066-7
5. Yilmaz G, Granger DN. Cell adhesion molecules and ischemic stroke. *Neurol Res*. 2008;30:783–793. doi:10.1179/174313208X341085
6. Tang C, Wang C, Zhang Y, et al. Recognition, Intervention, and monitoring of neutrophils in acute ischemic stroke. *Nano Lett*. 2019;19:4470–4477. doi:10.1021/acs.nanolett.9b01282
7. Zhang CY, Dong X, Gao J, Lin W, Liu Z, Wang Z. Nanoparticle-induced neutrophil apoptosis increases survival in sepsis and alleviates neurological damage in stroke. *Sci Adv*. 2019;5:eaax7964. doi:10.1126/sciadv.aax7964
8. Pu Z, Ma S, Wang L, et al. Amyloid-beta degradation and neuroprotection of dauricine mediated by unfolded protein response in a Caenorhabditis elegans model of Alzheimer's disease. *Neuroscience*. 2018;392:25–37. doi:10.1016/j.neuroscience.2018.09.022
9. Wang K, Wang L, Chen L, et al. Intranasal administration of dauricine loaded on graphene oxide: multi-target therapy for Alzheimer's disease. *Drug Deliv*. 2021;28:580–593. doi:10.1080/10717544.2021.1895909
10. Li M, Liu G, Wang K, et al. Metal ion-responsive nanocarrier derived from phosphonated calix[4]arenes for delivering dauricine specifically to sites of brain injury in a mouse model of intracerebral hemorrhage. *J Nanobiotechnol*. 2020;18:61. doi:10.1186/s12951-020-00616-3
11. Li YH, Gong PL. Neuroprotective effects of dauricine against apoptosis induced by transient focal cerebral ischaemia in rats via a mitochondrial pathway. *Clin Exp Pharmacol Physiol*. 2007;34:177–184. doi:10.1111/j.1440-1681.2007.04569.x
12. Wang L, Pu Z, Li M, Wang K, Deng L, Chen W. Antioxidative and antiapoptosis: neuroprotective effects of dauricine in Alzheimer's disease models. *Life Sci*. 2020;243:117237. doi:10.1016/j.lfs.2019.117237
13. Yang XY, Jiang SQ, Zhang L, Liu QN, Gong PL. Inhibitory effect of dauricine on inflammatory process following focal cerebral ischemia/reperfusion in rats. *Am J Chin Med*. 2007;35:477–486. doi:10.1142/S0192415X07004990
14. Dong PL, Han H, Zhang TY, Yang B, Wang QH, Eerdun GW. P-glycoprotein inhibition increases the transport of dauricine across the blood-brain barrier. *Mol Med Rep*. 2014;9:985–988. doi:10.3892/mmr.2013.1880
15. Meng H, Zhao H, Cao X, et al. Double-negative T cells remarkably promote neuroinflammation after ischemic stroke. *Proc Natl Acad Sci USA*. 2019;116:5558–5563. doi:10.1073/pnas.1814394116
16. Yang XY, Liu QN, Zhang L, Jiang SQ, Gong PL. Neuroprotective effect of dauricine after transient middle cerebral artery occlusion in rats: involvement of Bcl-2 family proteins. *Am J Chin Med*. 2010;38:307–318. doi:10.1142/S0192415X10007865
17. Egashira Y, Suzuki Y, Azuma Y, et al. The growth factor progranulin attenuates neuronal injury induced by cerebral ischemia-reperfusion through the suppression of neutrophil recruitment. *J Neuroinflammation*. 2013;10:105. doi:10.1186/1742-2094-10-105
18. Zhang Z, Cao X, Bao X, Zhang Y, Xu Y, Sha D. Cocaine- and amphetamine-regulated transcript protects synaptic structures in neurons after ischemic cerebral injury. *Neuropeptides*. 2020;81:102023. doi:10.1016/j.npep.2020.102023
19. Wu N, Zhang X, Bao Y, Yu H, Jia D, Ma C. Down-regulation of GAS5 ameliorates myocardial ischaemia/reperfusion injury via the miR-335/ROCK1/AKT/GSK-3beta axis. *J Cell Mol Med*. 2019;23:8420–8431. doi:10.1111/jcmm.14724

20. Cen J, Liu L, Li MS, et al. Alteration in P-glycoprotein at the blood-brain barrier in the early period of MCAO in rats. *J Pharm Pharmacol*. 2013;65:665–672. doi:10.1111/jphp.12033
21. Meng H, Fan L, Zhang CJ, et al. Synthetic VSMCs induce BBB disruption mediated by MYPT1 in ischemic stroke. *iScience*. 2021;24:103047. doi:10.1016/j.isci.2021.103047
22. Chen J, Sanberg PR, Li Y, et al. Intravenous administration of human umbilical cord blood reduces behavioral deficits after stroke in rats. *Stroke*. 2001;32:2682–2688. doi:10.1161/hs1101.098367
23. Zhang MJ, Sun JJ, Qian L, et al. Human umbilical mesenchymal stem cells enhance the expression of neurotrophic factors and protect ataxic mice. *Brain Res*. 2011;1402:122–131. doi:10.1016/j.brainres.2011.05.055
24. Alamri FF, Shoyaib AA, Biggers A, Jayaraman S, Guindon J, Karamyan VT. Applicability of the grip strength and automated von Frey tactile sensitivity tests in the mouse photothrombotic model of stroke. *Behav Brain Res*. 2018;336:250–255. doi:10.1016/j.bbr.2017.09.008
25. Chen J, Jin J, Zhang X, et al. Microglial lnc-U90926 facilitates neutrophil infiltration in ischemic stroke via MDH2/CXCL2 axis. *Mol Ther*. 2021;29:2873–2885. doi:10.1016/j.ymthe.2021.04.025
26. Wang Y, Jin H, Wang W, Wang F, Zhao H. Myosin1f-mediated neutrophil migration contributes to acute neuroinflammation and brain injury after stroke in mice. *J Neuroinflammation*. 2019;16:77. doi:10.1186/s12974-019-1465-9
27. Deng Y, Herbert JA, Smith CM, Smyth RL. An in vitro transepithelial migration assay to evaluate the role of neutrophils in Respiratory Syncytial Virus (RSV) induced epithelial damage. *Sci Rep*. 2018;8:6777. doi:10.1038/s41598-018-25167-4
28. Seeliger D, de Groot BL. Ligand docking and binding site analysis with PyMOL and Autodock/Vina. *J Comput Aided Mol Des*. 2010;24:417–422. doi:10.1007/s10822-010-9352-6
29. Perez-de-puig I, Miro-Mur F, Ferrer-Ferrer M, et al. Neutrophil recruitment to the brain in mouse and human ischemic stroke. *Acta Neuropathol*. 2015;129:239–257. doi:10.1007/s00401-014-1381-0
30. Zhou YX, Wang X, Tang D, et al. IL-2mAb reduces demyelination after focal cerebral ischemia by suppressing CD8(+) T cells. *CNS Neurosci Ther*. 2019;25:532–543. doi:10.1111/cns.13084
31. Chauhan A, Hudobenko J, Al Mamun A, et al. Myeloid-specific TAK1 deletion results in reduced brain monocyte infiltration and improved outcomes after stroke. *J Neuroinflammation*. 2018;15:148. doi:10.1186/s12974-018-1188-3
32. Kim SW, Davaanyam D, Seol SI, Lee HK, Lee H, Lee JK. Adenosine triphosphate accumulated following cerebral ischemia induces neutrophil extracellular trap formation. *Int J Mol Sci*. 2020;21:7668.
33. Kessenbrock K, Frohlich L, Sixt M, et al. Proteinase 3 and neutrophil elastase enhance inflammation in mice by inactivating antiinflammatory progranulin. *J Clin Invest*. 2008;118:2438–2447. doi:10.1172/JCI34694
34. Chen C, Liu P, Wang J, et al. Dauricine attenuates spatial memory impairment and Alzheimer-like pathologies by enhancing mitochondrial function in a mouse model of Alzheimer's disease. *Front Cell Dev Biol*. 2020;8:624339. doi:10.3389/fcell.2020.624339
35. Peng C, Fu X, Wang K, et al. Dauricine alleviated secondary brain injury after intracerebral hemorrhage by upregulating GPX4 expression and inhibiting ferroptosis of nerve cells. *Eur J Pharmacol*. 2021;914:174461. doi:10.1016/j.ejphar.2021.174461
36. Wang X, Liu Y, Sun Y, Liu W, Jin X. Blood brain barrier breakdown was found in non-infarcted area after 2-h MCAO. *J Neurol Sci*. 2016;363:63–68. doi:10.1016/j.jns.2016.02.035
37. Dziennis S, Akiyoshi K, Subramanian S, Offner H, Hurn PD. Role of dihydrotestosterone in post-stroke peripheral immunosuppression after cerebral ischemia. *Brain Behav Immun*. 2011;25:685–695. doi:10.1016/j.bbi.2011.01.009
38. Wolinski P, Glabinski A. Chemokines and neurodegeneration in the early stage of experimental ischemic stroke. *Mediators Inflamm*. 2013;2013:727189. doi:10.1155/2013/727189
39. Assem S, Abdelbaki TN, Mohy-El Dine SH, Ketat AF, Abdelmonsif DA. SERPINE-1 gene methylation and protein as molecular predictors of laparoscopic sleeve gastrectomy outcome. *Obes Surg*. 2020;30:2620–2630. doi:10.1007/s11695-020-04533-0
40. Kortlever RM, Higgins PJ, Bernards R. Plasminogen activator inhibitor-1 is a critical downstream target of p53 in the induction of replicative senescence. *Nat Cell Biol*. 2006;8:877–884. doi:10.1038/ncb1448
41. Jiang C, Liu G, Luckhardt T, et al. Serpine 1 induces alveolar type II cell senescence through activating p53-p21-Rb pathway in fibrotic lung disease. *Aging Cell*. 2017;16:1114–1124. doi:10.1111/acel.12643
42. Marchand A, Proust C, Morange PE, Lompre AM, Tregouet DA, Chadwick BP. miR-421 and miR-30c inhibit SERPINE 1 gene expression in human endothelial cells. *PLoS One*. 2012;7:e44532. doi:10.1371/journal.pone.0044532